

# Effect of precursor history on synthesis of high- $T_c$ BPSCCO superconductor

HANJIN LIM, J. G. BYRNE

*Department of Metallurgical Engineering, 412 WBB, University of Utah, Salt Lake City, UT 84112, USA*

High- $T_c$  lead-doped BSCCO superconductors (BPSCCO) were prepared from precursors of three different histories. The method, which combined three kinds of calcined powders, decreased the total sintering time for the formation of high- $T_c$  BPSCCO superconductor phases relative to other methods based on one type of powder. The proportion of secondary phase, such as  $\text{Ca}_2\text{CuO}_3$  was also reduced. As a result, the transition temperature,  $T_c$ , from the current method is higher than for the latter fabrication methods. The  $c$ -axis parameters of BSCCO superconductors from different precursors were compared. The average X-ray particle size of each phase in the bulk sample was calculated from the Scherrer formula. Finally, the surface morphology and composition of BPSCCO were examined by SEM and energy dispersive spectrometry.

## 1. Introduction

The homological series of the bismuth-based copper oxides of the general formula  $\text{Bi}_2\text{Sr}_2\text{Ca}_{n-1}\text{Cu}_n\text{O}_{2n+4}$  (BSCCO) represents an important group of high-temperature superconductors (HTS). They are widely studied from the fundamental point of view as well as with regard to their potential applications. Several superconducting phases can be obtained from these oxides depending on the preparation conditions [1]. These phases are the following: Bi: Sr: Ca: Cu = 2:2:0:1 ( $T_c \sim 22$  K); 2:2:1:2 ( $T_c \sim 80$  K), and 2:2:2:3 ( $T_c \sim 105$  K). It has also been observed that mixtures of these phases are usually obtained. Some techniques have been elaborated, aiming to purify the materials and select the highest proportion of the 2:2:2:3 phase [2, 3].

With controlled lead concentration added as a dopant, it was reported that one can easily synthesize the HTS powder and stabilize the 2223 phase [4, 5]. However, there is still some controversy on the detailed technique and even on the nature of the doped ceramics. It is generally difficult to obtain monophase compositions due to various factors. Both thermodynamic and kinetic factors are clearly involved in determining the ease of formation as well as phase purity of these cuprates. BSCCO 2201 is said to be stable around 810 °C, BSCCO 2212 around 840 °C, and BSCCO 2223 close to the melting point (850 °C) after heating for several days or even weeks [6]. Of all the members of the BSCCO family, the  $n = 2$  members (2212) seems to be the most stable. It was reported that the 2212 phase exhibited an extended single-phase region having variable Sr/Ca ratio and bismuth content. With increasing temperature, the single-phase region shrinks and moves to a strontium-rich composition [7]. The formation of 2223 is accel-

erated by the presence of a transient liquid [8–12]. The liquid also heals damage done during mechanical processing and facilitates grain growth and texturing [8]. The source of the liquid remains in question, but probably depends on the exact powder-processing scheme. Some workers believe that 2223 forms by a reaction between the liquid and 2212 [8, 9]. Others suggest that 2212 melts during the formation of 2223 and that 2223 formation is most favourable when the melting point of 2212 is lower than that of 2223 [10–12]. Processing in reduced oxygen partial pressure [8], and making 2212 that is rich in calcium [11], were suggested to obtain a low-melting 2212 phase. Recently, better control of the formation of 2223 by reducing other phases present was reported by a two-powder process that manipulates the partial-melting behaviour through mixing BSCCO 2212 and (Sr,Ca)  $\text{CuO}_2$  separately [13].

## 2. Experimental procedure

Reagent-grade  $\text{Bi}_2\text{O}_3$ ,  $\text{PbO}$ ,  $\text{SrCO}_3$ ,  $\text{CaCO}_3$  and  $\text{CuO}$  powders were combined with cation stoichiometries of Bi: Pb: Sr: Ca: Cu = 1.8–1.85: 0.35–0.40: 1.8–2.1: 1.9–2.2: 3.0–3.05. Powders were ball-milled over 16 h with isopropanol and  $\text{ZrO}_2$  grinding media (wet mixing), or just with grinding media (dry mixing). The mixed powders were calcined twice in air or a reduced oxygen atmosphere. Three types of precursors were prepared from these powders. The precursor for the sample called bulk1 was made by combining the three kinds of calcined powders, hereafter called the three-powder process. The precursors called bulk2 and bulk3 were made from one calcined powder. Each precursor was examined by X-ray diffraction (XRD) for phase identification and particle size. The latter

was determined by X-ray diffraction using the Scherrer formula [14]

$$t = \frac{0.9\lambda}{B \cos \theta_B} \quad (1)$$

where  $B$  is the angular peak width converted to radians,  $\lambda$  is the characteristic wavelength of copper (0.154 nm), and  $\theta_B$  is the Bragg angle of the peak. The following simple equation was used to determine  $B$

$$B^2 = B_M^2 - B_S^2 \quad (2)$$

where  $B_S$  is the measured breadth in degrees of  $2\theta_B$ , at half-maximum intensity, of a line from the standard close to  $\theta_B$  of the sample peak, and  $B_M$  is the measured breadth at half maximum intensity of the peak from the sample. As the standard, a silicon single crystal was used. Nickel-filtered copper radiation was used throughout.

Precursors were pressed into pellets of 28 mm diameter and about 2 mm thick and sintered at 840 °C for 80 h in a 10% O<sub>2</sub> atmosphere. Between each sintering, pellets were re-ground with an Al<sub>2</sub>O<sub>3</sub> mortar and pestle and re-pressed. Each bulk sample was sintered several times until mainly BSCCO 2223 phase resulted. XRD utilized CuK<sub>α</sub> over a 2θ range from 3°–59°.  $T_c$  was measured by a four-probe method: the sample was spark-bonded or silver pasted with gold wires, and then annealed at 800 °C for 2 h in an oxygen atmosphere to reduce the contact resistance. To study the surface morphology and composition of the sample, scanning electron microscopy (SEM) and energy-dispersive spectrometry (EDS) were utilized.

### 3. Results and discussion

Table I shows the conditions and phases for each powder synthesis. The bulk1 sample was made by combining ExpIII-2, ExpIII-3 and ExpV. The ExpIII-3 was calcined further at 850 °C for 48 h after ExpIII-2 was taken. The bulk2 sample was made from ExpIV-2, and the bulk3 sample from ExpVI. In the three-powder process for the bulk1 sample, the major phase in the calcined powder was BSCCO 2212. CaO, CuO,

and Ca<sub>2</sub>CuO<sub>3</sub> were also still present in the powder. The precursor for the bulk2 sample contained BSCCO 2212 and Ca<sub>2</sub>CuO<sub>3</sub> as major phases. The precursor for the bulk3 sample also had BSCCO 2212 and Ca<sub>2</sub>CuO<sub>3</sub> as major phases, and BSCCO 2223 pre-existed in the powder as a minor component.

To obtain mainly BSCCO 2223 phase in these bulk samples, each bulk sample was heat treated at 840 °C in 10% oxygen for different sintering times. XRD patterns are shown in Fig. 1. In the bulk1 sample, Bi<sub>2-x</sub>Pb<sub>x</sub>Sr<sub>2</sub>Ca<sub>2</sub>Cu<sub>3</sub>O<sub>y</sub> (BPSCCO 2223) was the major phase, and Ca<sub>2</sub>CuO<sub>3</sub> remained as a minor component. In the three-powder process, total sintering time to obtain BSCCO 2223 decreased to a value of 160 h. In contrast, the bulk2 sample was mostly converted to BSCCO 2223 from the remaining BSCCO 2212 only after a very long sintering time of 430 h with some BSCCO 2212 remaining. The increase of BSCCO 2223 over BSCCO 2212 was obtained after 270 h sintering at the same condition in the bulk3 sample, but a relatively large amount of Ca<sub>2</sub>CuO<sub>3</sub> still remained. In general, the longer the sintering steps, the more BSCCO 2212 was converted into BSCCO 2223.

The  $c$ -axis of the lattice was measured from (00 $l$ ) peaks in X-ray diffraction patterns. In general, the lattice structure of the BSCCO superconductor is known as orthorhombic, where the  $d$ -spacing is

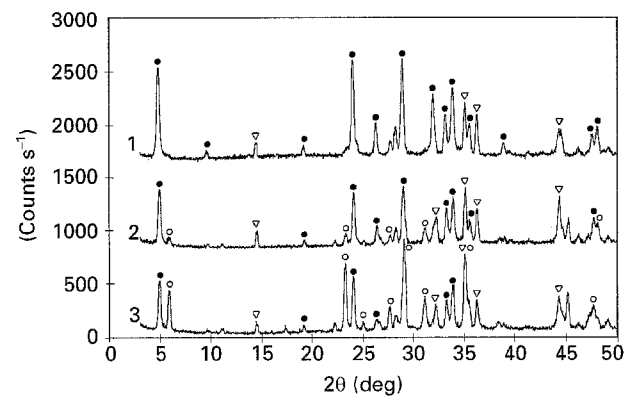


Figure 1 X-ray diffraction patterns of (●) BSCCO 2223, (○) BSCCO 2212 and (▽) Ca<sub>2</sub>CuO<sub>3</sub> for (1) bulk1, (2) bulk2, and (3) bulk3 samples.

TABLE I Summary of precursor syntheses

	Bi/Pb/Sr/Ca/Cu	Mixing method	First calcining temp.(°C)	Final calcining temp.(°C)	Additional calcining temp.(°C)	Atmosphere	Major phases	Minor phases
ExpIII-2	1.85/0.35/1.9/2.05/3.05	wet	835	845		Nitrogen/air	BSCCO 2212	CaO + CuO
ExpIII-3	1.85/0.35/1.9/2.05/3.05	wet			850(48 h)	Air	BSCCO 2212	Ca <sub>2</sub> CuO <sub>3</sub>
ExpIV-2	1.85/0.4/1.95/2.05/3.05	dry	835	845		Nitrogen/air	BSCCO 2212 + Ca <sub>2</sub> CuO <sub>3</sub>	
ExpV	1.85/0.35/2.1/1.9/3.05	wet	800	835		Air/10% oxygen	BSCCO 2212	Ca <sub>2</sub> CuO <sub>3</sub> + CuO
ExpVI	1.8/0.4/1.8/2.2/3.0	wet	835	840	840(80 h)	Nitrogen/10% oxygen	BSCCO 2212 + Ca <sub>2</sub> CuO <sub>3</sub>	BSCCO 2223

determined as follows

$$\frac{1}{d^2} = \frac{h^2}{a^2} + \frac{k^2}{b^2} + \frac{l^2}{c^2} \quad (3)$$

In the case of the (00*l*) peak

$$\frac{l^2}{d^2} = \frac{l^2}{c^2} \quad (4)$$

Therefore

$$l = \frac{c}{d} \quad (5)$$

The *c*-axis is easily determined by the slope between 1 and 1/*d*. Table II shows the *c*-axis of both BSCCO

TABLE II The *c*-axis parameter of each sample

Sample	Sintering steps	<i>c</i> -axis of 2223 (nm)	<i>c</i> -axis of 2212 (nm)
Bulk1	1	3.7147	
	2	3.7153	
Bulk2	1		3.0722
	2		3.0752
	3	3.7192	3.0764
	4	3.7178	3.0771
	5	3.7225	3.0843
Bulk3	1	3.7187	3.0781
	2	3.7173	3.0777
	3	3.7177	3.0782

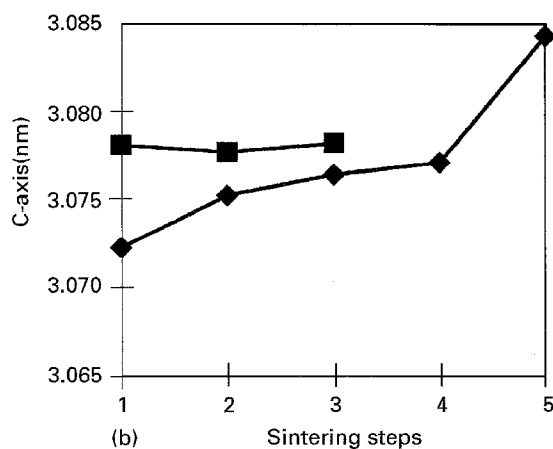
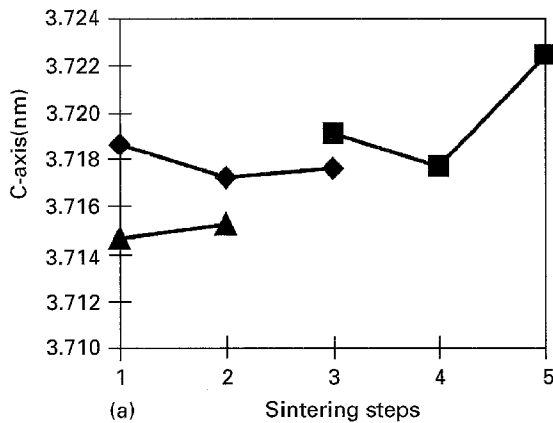


Figure 2 The *c*-axis parameters of BSCCO (a) 2223 and (b) 2212 in the bulk samples according to the sintering steps. (a)  $\blacklozenge$  bulk3,  $\blacksquare$  bulk2,  $\blacktriangle$  bulk1; (b)  $\blacklozenge$  bulk2;  $\blacksquare$  bulk3.

2223 and BSCCO 2212 according to the sintering process. The *c*-axis for both superconducting phases increased in the final sintering step compared to the first step, with the exception of the bulk3 sample (Fig. 2) where it was constant or decreased slightly. Apparently, pre-existing BSCCO 2223 from the precursor gave a negative effect in making a bulk sample. The bulk2 sample showed the largest *c*-axis of BSCCO 2223, but still contained unconverted BSCCO 2212 whose *c*-axis gradually increased with sintering time.

The critical transition temperature,  $T_c$ , for each bulk sample was measured by a four-probe resistance method. The bulk1, bulk2, and bulk3 samples showed the transition at 102, 78 and 88 K, respectively. The reason that the bulk2 and bulk3 samples had a transition at lower temperatures is probably due to the residual  $\text{Ca}_2\text{CuO}_3$  secondary phase or incomplete conversion of BSCCO 2212 to BSCCO 2223 phase [15]. Even though the *c*-axis is larger in the bulk2 sample than in any other bulk samples,  $T_c$  was lower in the bulk2 sample because of larger amounts of  $\text{Ca}_2\text{CuO}_3$  and unconverted BSCCO 2212 present.

The three-powder process accelerated the conversion of BSCCO 2212 from precursor into BSCCO 2223 with the highest  $T_c$  superconducting phase in the BSCCO family. As a result, the bulk1 sample had a higher transition temperature compared to both bulk2 and bulk3 samples although the *c*-axis of BSCCO 2223 was the lowest. From these results, it is concluded that purifying the superconducting phase, especially BSCCO 2223, is important to improve superconductivity, and depends greatly on the history of the powder processing.

Fig. 3 shows the average X-ray particle size of the secondary phase ( $\text{Ca}_2\text{CuO}_3$ ) and the BSCCO 2223

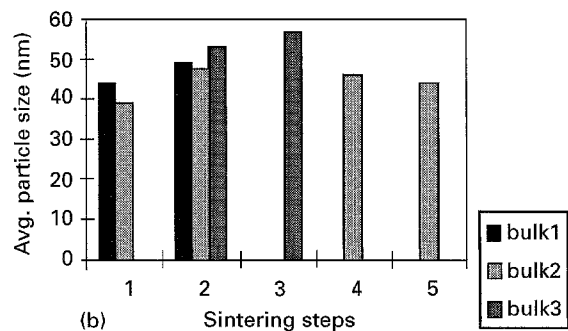
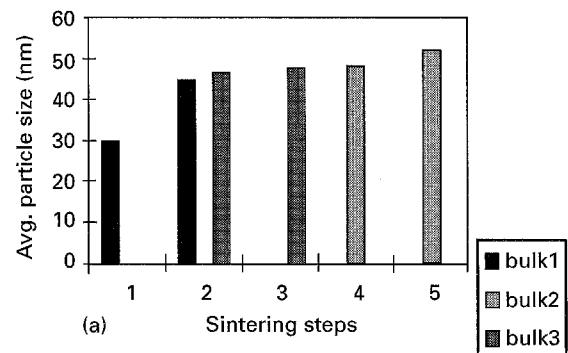


Figure 3 The average particle sizes of (a) BSCCO 2223 and (b) the secondary phase ( $\text{Ca}_2\text{CuO}_3$ ) in the bulk samples according to the sintering steps.

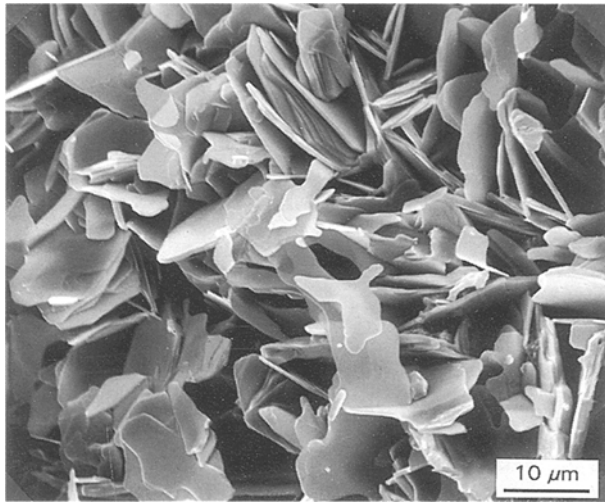


Figure 4 Scanning electron micrograph showing the micaceous morphology typical of the BSCCO 2223 phase in the bulk1 sample.

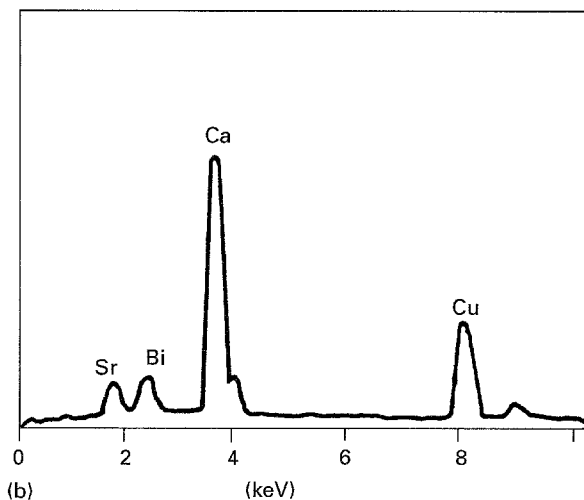
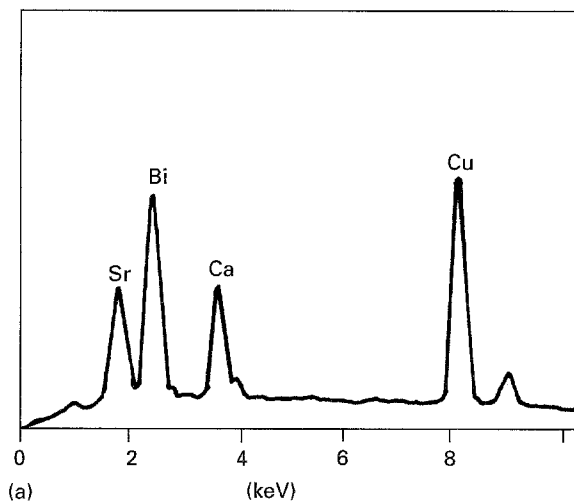


Figure 5(a) Chemical analysis for BSCCO superconductor phase in the bulk1 sample by energy dispersive spectrometry (EDS). (b) Chemical analysis for  $\text{Ca}_2\text{CuO}_3$  phase in the bulk1 sample by EDS.

phase for the sintering steps for each bulk sample. Comparing the X-ray particle size of  $\text{Ca}_2\text{CuO}_3$  of bulk1 with that of bulk3, more coarse secondary phases are present in the bulk3 sample. This may result in the lower transition temperature for the bulk3 sample than that of the bulk1. As the sintering

time increased, the particle size of  $\text{Ca}_2\text{CuO}_3$  in the bulk2 sample increased up to the second sintering step, and then gradually decreased afterwards. In the case of the BSCCO 2223 phase, the particle size rapidly increased up to the second step of sintering, and afterwards gradually increased.

The typical micaceous morphology of the superconducting phase is shown in Fig. 4. Fig. 5 shows the clear delineation of EDS scans between (a) the BSCCO superconducting phase and (b) the  $\text{Ca}_2\text{CuO}_3$  phase.

#### 4. Conclusions

1. The high- $T_c$  lead-doped BSCCO superconductor was made from precursors of different histories. The superconducting phases were highly dependent on powder processing.

2. With the three-powder process, which combined three kinds of calcined-powders for the precursor, the formation of BSCCO superconductor was accelerated, and secondary phases such as  $\text{Ca}_2\text{CuO}_3$  were reduced.

3. The transition temperature,  $T_c$  of the superconductor from the three-powder process is higher than that from the one-powder process.

#### Acknowledgement

This research was supported by Mineral Leasing funds from the College of Mines and Earth Sciences at the University of Utah.

#### References

1. H. MAEDA, T. TENAKA, M. FUKUTOMI and T. TASANO, *Jpn. J. Appl. Phys.* **27** (1988) L209.
2. H. U. HABERMEIER, W. SOMMER, and G. MERTENS, in "Science and Technology in Thin-Film Superconductors", edited by R. D. McConnell and S. A. Wolf (Plenum, New York, 1989) p. 131.
3. T. KANAI, T. KAMO, and S. MATSUDA, *Supercond. Sci. Technol.* **4** (1991) 207.
4. R. J. CAVA *et al.* *Phys. C* **155** (1988) 560.
5. M. TANAKA *et al.*, *Jpn J. Appl. Phys.* **27** (1988) L1041.
6. C. T. WU, K. C. GORETTA, M. T. LANAGAN, A. C. BIONDO, and R. B. POEPEL, in "Processing of Long Lengths of Superconductors", edited by U. Balachandran *et al.* (TMS, Pittsburgh, PA, 1993) p. 101.
7. P. MAJEWSKI, H.-L. SU and B. HETTICH, *Adv. Mater.* **4** (1992) 508.
8. Y. YAMADA, B. OBST and R. FLUKIGER, *Supercond. Sci. Technol.* **4** (1991) 165.
9. S. SOO OH and K. OSAMURA, *ibid.* **4** (1991) 239.
10. K. AOTA, H. HATTORI, T. HATANO, K. NAKAMURA and K. OGAWA, *Jpn J. Appl. Phys.* **28** (1989) L2196.
11. J. TSUCHIYA, H. ENDO, N. KIJIMA, A. SUMIYAMA, M. MIZUNO and Y. OGURI, *ibid.* **29** (1989) L1918.
12. T. HATANO, K. AOTA, S. IKEDA, K. NAKAMURA and K. OGAWA, *ibid.* **27** (1988) L2055.
13. S. E. DORRIS, B. C. PROROK, M. T. LANAGAN, S. SINHA and R. B. POEPEL, *Phys. C* **212** (1993) 66.
14. B. D. CULLITY, "Elements of X-Ray Diffraction", 2nd edn. (Addison-Wesley, Reading, MA, 1978).
15. A. UMEZAWA, Y. FENG, H. S. EDELMAN, Y. E. HIGH, D. C. LARBALESTIER, Y. S. SUNG and E. E. HELSTROM, *Phys. C* **198** (1992) 261.

Received 28 April  
and accepted 25 October 1995